ERDC TN-SWWRP-12-1
August 2012

Storm Drain Effects on Urban Flooding

by Fred L. Ogden, Ph.D., P. E., Justin M. Niedzialek, Ph.D., and Aaron R. Byrd, P. E.

PURPOSE: To describe the new storm drainage network model in the hydrologic model Gridded Surface Subsurface Hydrologic Analysis (GSSHA) (Downer et al. 2006) and demonstrate the effects of storm drainage networks on flooding in urban areas.

Abstract. Urban flooding is a primary concern in all developed areas. Understanding what factors contribute to the magnitude and frequency of flooding is of primary importance when designing an engineering system to mitigate flooding. To understand the effect of impervious area versus the role of the storm drainage system in urban flooding, the U.S. Army Corps of Engineers Gridded Surface Subsurface Hydrologic Analysis model was enhanced with a subsurface drainage model. The subsurface drainage model is described and an example application in Maryland of an urban area demonstrated that the storm drainage system plays a major role in the hydrologic response of a watershed to moderate-to-high rainfall events. Due to the under-capacity of the storm drainage system, however, the effect of the storm drainage network for extreme rainfall events is greatly diminished.

Forward and Acknowledgments. Much of the storm drainage model development and theory is taken directly from Ji (1998). The applications section was taken largely from Jonathan Zahner's M.S. thesis (Zahner 2004), and is provided as an example.

Introduction. There is no argument that flood magnitude and frequency increase as urban development spreads throughout a watershed. It is obvious that understanding this trend is of great social and economic importance but what causes this change in hydrology is the source of much debate and numerous studies. Changes in urban runoff volume and flood peaks have been blamed historically on increases in impervious area. This theory was recently challenged by a study in and around Charlotte, North Carolina (Smith et al. 2002). The conclusion by Smith et al. (2002) was that the increase in storm drainage connectivity and hence hydraulic efficiency played the greatest role in increasing flood magnitudes. The inability to explicitly simulate storm drainage networks is seen as a major limitation in the application of GSSHA to urbanized areas. To address this issue, the SUPERLINK (Ji 1998) storm drainage scheme was added to GSSHA (Zahner 2004).

SUPERLINK BACKGROUND. A complete review of the literature was undertaken to find a robust method that would allow integration with the advanced features of GSSHA. The USGS Full Equations (FEQ) model (Franz et al. 1997), U.S. National Weather Service DWOPER (Lewis et al. 1996), SWMM (Rossman et al. 2004), Danish Hydraulics Institute MOUSE (Gustafsson et al. 1999), and the SUPERLINK scheme (Ji 1998) were all evaluated. For a more

complete review of the methods used to evaluate which model was most appropriate for GSSHA, the reader is referred to Zahner (2004).

Of these schemes, SUPERLINK was judged the most capable and the literature contained a detailed description of the formulation to allow a GSSHA implementation. Although it has not had the widespread use and acceptance as many of the other models, Ji (1998) tested this scheme on a complex data set from the city of Winnipeg, Manitoba, Canada. Winnipeg, located on the banks of the Red River of the North, is a very low gradient watershed (subject to backwater effects and surcharging) and contains multiple looped and branched pipes. Ji (1998) compared SUPERLINK output to both SWMM Extran and physical observations, with favorable results against both. SUPERLINK was stable at a 400 second time step, compared to a 7 second Extran time step, and generated mass conservation errors of only 0.32 percent over a 5-hour simulation period. Based on the comprehensive formulation and satisfactory simulation results, SUPERLINK was chosen as the pipe network model to couple with GSSHA.

SUPERLINK THEORY AND INTEGRATION. *Superlinks* are series of links connecting junctions, and must have a junction on either end. A *junction* is defined as a point where two or more superlinks meet, or the unconnected end of a superlink (such as intake/discharge point of network). A *link* is a segment of a superlink connecting two nodes, and a *node* is a computational point in a superlink. The use of both nodes and links may seem redundant, but in fact is quite integral to the "staggered grid" technique employed in SUPERLINK and is discussed later in detail. Figure 1 illustrates the nomenclature.

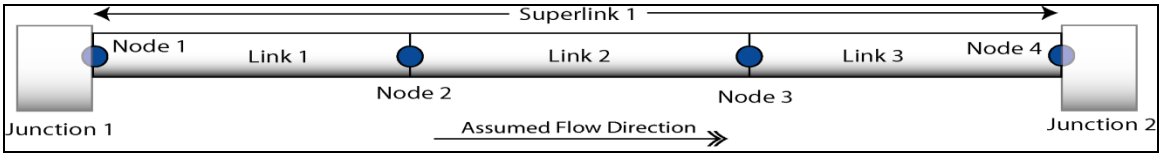

Figure 1. SUPERLINK junction, link, and node nomenclature.

Inflow is allowed at junctions and nodes via two primary structures. The first is a culvert, which captures a natural stream channel, and is possible only at a junction. The second is any type of grate/curb opening in a roadway, and is possible at either a junction or a node. Discharge can occur from a flooded manhole, drop inlet, or an outlet pipe (node or junction), and junctions may discharge directly into a channel. The parameters for these inlets and outlets are contained in the node and junction cards defined in the file format.

Modeling Theory. The central equations solved in this model are the conservation of mass (or continuity equation) (1) and the de St. Venant equation of motion (2). This pair of nonlinear partial differential equations take the form of:

$$\frac{\partial A}{\partial t}+\frac{\partial Q}{\partial x}=q_0 \tag{1}$$

$$\frac{\partial Q}{\partial t}+\frac{\partial Qu}{\partial x}+gA\left(\frac{\partial h}{\partial x}-S_0+S_f+S_L\right)=0 \tag{2}$$

where A = flow cross-sectional area, Q = discharge, h = depth, u = velocity, S_0 = bed slope of conduit, S_f = friction head loss slope, S_L = local head loss slope, q_0 = lateral flow to conduit, g = gravitational constant, x = distance, and t = time.

The two fundamental equations (1 & 2) are applied on sections of a conduit segmented by computational nodes. Conservation of mass is represented by Equation 1, and is applied across a node. The staggered grid approach requires the conservation of momentum Equation 2 to be applied on a different control volume. The layout of these volumes is shown in Figure 2.

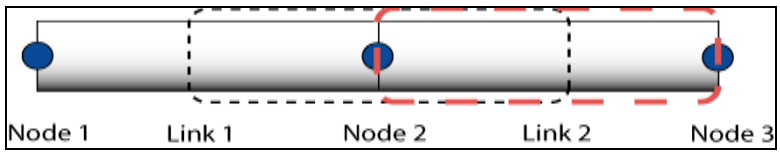

Figure 2. SUPERLINK staggered grid computational scheme.

The control volume shown in short dashes illustrates the continuity equation for node 2, while the long dashed envelope indicates the momentum equation for link 2.

The St. Venant equations of motion only apply to free surface flow. During intense events, subsurface systems commonly flow full and under pressure. A common solution is to employ the "Priessmann slot" to extend the free surface equations to conduits flowing full. This slot area is not used for flow calculations, but merely to pressurize the conduit still being modeled by open channel flow equations.

Linearized Equations. To solve the partial differential equations, they must be discretized over their respective control volumes. Thus, unsteady terms such as flow rate and depth become time dependent variables. The discretized continuity equation with indices referring to Figure 2 becomes

$$Q_2^{t+\Delta t} - Q_1^{t+\Delta t} + \left(\frac{B_2\Delta x_2}{2} + \frac{B_1\Delta x_1}{2} + A_{S1}\right)\frac{h_2^{t+\Delta t} - h_2^{t}}{\Delta t} = Q_{01} \tag{3}$$

The momentum equation takes a similar form

$$\begin{aligned}\left(Q_2^{t+\Delta t} - Q_2^{t}\right)\left(\frac{\Delta x_2}{\Delta t}\right) + x_3 Q_3^{t+\Delta t} - x_2 Q_2^{t+\Delta t} + gA_2\left(S_{f2} + S_{L2}\right)\Delta x \\ = gA_2 S_{02}\Delta x + gA_2\left(h_2^{t+\Delta t} - h_3^{t+\Delta t}\right)\end{aligned} \tag{4}$$

The only new term in these equations is B, the top width of flow area. Subscripts refer to the link or node number, and superscripts denote either the current or future time step (current if not marked).

Boundary Conditions. As with any modeling problem, a set of boundary conditions must be applied to the extents of the network. With regards to the SUPERLINK model, these boundaries are located at the ends of each superlink, or junctions. The first component of the junction

boundary is the water surface elevation (head). Junction heads may be known or unknown, as determined by the actual network configuration. A known junction head may be controlled by something external to the model, such as a reservoir at the network outlet. This feature would create backwater pressure propagating upstream, thus affecting flow upstream. Unknown head boundary conditions occur at internal connections of two or more superlinks. Junctions representing an intake structure at the start of a superlink could also have an unknown head.

Flow into and out of these junctions, whether of known or unknown head, is governed by end condition boundary equations. Inlet entrance geometry governs pipeflow in steep channels, and exit properties can control in low gradient conditions. The end equations use the head in the junction as well as geometric variables to produce a set of coefficients for each inlet and outlet. The inlet and outlet coefficients by Ji (1998) were found to be unstable in certain situations and were reformulated as discussed in the model development section.

Solution Technique. The implicit scheme is defined by a simultaneous solution to all unknowns in the system at each time step. Instead of computing the head at every internal point (junctions and nodes) as the model steps through time, only unknown junctions are part of the solution matrix. The reduction in the matrix size and thus computational demand is substantial. But the elegance of this routine is the way in which the unknown internal node depth and flow are incorporated into the junction matrix solution. Through a series of recurrence relations, the momentum and continuity equations are propagated throughout each superlink from one node to the next. This is done in both the forward and reverse directions to capture both positive and negative flow. The resulting coefficients become part of a relatively complex equation relating junction heads, superlink end conditions, internal node depth, internal pipe flow rate, and current timestep network inputs. Full details of the SUPERLINK scheme are presented in Ji (1998).

The matrix used to solve these equations takes the form as shown, and typically can exceed 200 x 200 in size.

$$\begin{bmatrix} F_{1,1} & \Phi & 0 & 0 \\ 0 & F_{2,2} & \Phi & 0 \\ 0 & \psi & F_{3,3} & \psi \\ 0 & \psi & 0 & F_{4,4} \end{bmatrix} \begin{bmatrix} H_1 \\ H_2 \\ H_3 \\ H_4 \end{bmatrix} = \begin{bmatrix} G_1 \\ G_2 \\ G_3 \\ G_4 \end{bmatrix} \tag{5}$$

In this matrix, three main components are represented. First, the square matrix set is clearly of a sparse nature, but randomly so. The diagonal elements denoted by F and off-diagonal elements Φ and ψ all are summations of Superlink coefficients (Equations 30-33, Ji, 1998). The second variable, H, is a one-dimensional array of heads at the future time step for each junction in the network. Third is the "right hand side" vector of the matrix equation. G is composed of values from the current time step including junction head and boundary conditions, as well as junction inflows for the future time step. With the matrix constructed, any number of solution techniques can be applied. A generalized Lower-Upper Triangle (LU) decomposition solution method was chosen, which provides a full solution of a sparse matrix.

Model Development for GSSHA.

SUPERLINK Algorithm. The superlink algorithm was coded from scratch from the algorithm published by Ji (1998). The following computational steps are required in the Ji (1998) solution algorithm:

1) Calculate momentum and continuity coefficients for a superlink;
2) Calculate forward recurrence relations for each node and link within the superlink;
3) Calculate reverse recurrence relations for each node and link within the superlink;
4) Calculate boundary condition coefficients;
5) Using all of the above coefficients and recurrence relations, calculate a set of coefficients for use in the solution matrix;
6) Repeat steps 1-5 for each superlink in the system;
7) Calculate matrix values based on connectivity of the superlinks;
8) Solve the sparse matrix;
9) Based on the matrix solution of head at each unknown junction, calculate the flow at the upper and lower ends of each superlink;
10) Solve for flow and depth in each pipe and node, respectively;
11) Continue from step 1 with new flows and depths.

Entrance hydraulics. The general equation for inlet-controlled flow is given as

$$Q = CA\sqrt{2g\Delta H} \tag{6}$$

where C is a geometric coefficient, A is the flow area, and ΔH is the difference in head between the supply reservoir (junction) and pipe (node 1, link 1). Because Ji (1998) had taken entrance boundary equations from other sources (and thus the derivation could not be followed easily.) we re-derived the superlink end equations from Equation 5 and created an alternate set of boundary conditions. We define $\Delta H = H - h - Z_{inv}$ where H is the junction head, h is the depth at the first node, and Z_{inv} is the invert elevation of the first node. By squaring both sides of the flow equation we get:

$$Q^2 = C^2 A^2 g\,(H - h - Z_{inv}) \tag{7}$$

The time varying Q is broken into the current time step and the future time step, and we solve for depth h, where $t+\Delta t$ it the future timestep. (Equation 8) This process can be applied to the downstream end of a pipe as well to account for instances of backward flow. (Equation 9)

$$h_u = \frac{|Q_u| Q_u^{\,t+\Delta t}}{C_u^{\,2} A_u^{\,2} g} + H_u - Z_{inv,u} \tag{8}$$

$$h_d = -\frac{|Q_d|Q_d^{t+\Delta t}}{C_d^{\,2} A_d^{\,2} g} + H_d - Z_{inv,d} \tag{9}$$

where the subscripts *u* and *d* refer to the depth either upstream or downstream.

Exit Hydraulics. Like the pipe entrances, pipe exits were modified from the Ji (1998) algorithm to more accurately model various flow regimes. In exit hydraulics, four possible conditions must be considered for pipes flowing less than full (see Figure 3). First, in a mild sloped channel where normal depth is greater than critical depth and junction head less than critical depth, the outfall depth is controlled by critical depth. Second, steep sloped channel exits where critical depth is greater than normal depth are governed at the exit by normal depth. Third is a critical sloped channel where normal depth equals critical depth, critical depth is used for end control. Fourth is the case of backwater effects, when the depth in the downstream junction begins to affect depths upstream. To simulate backwater effects, the head in the junction must exceed the head of critical depth (critical depth + invert elevation).

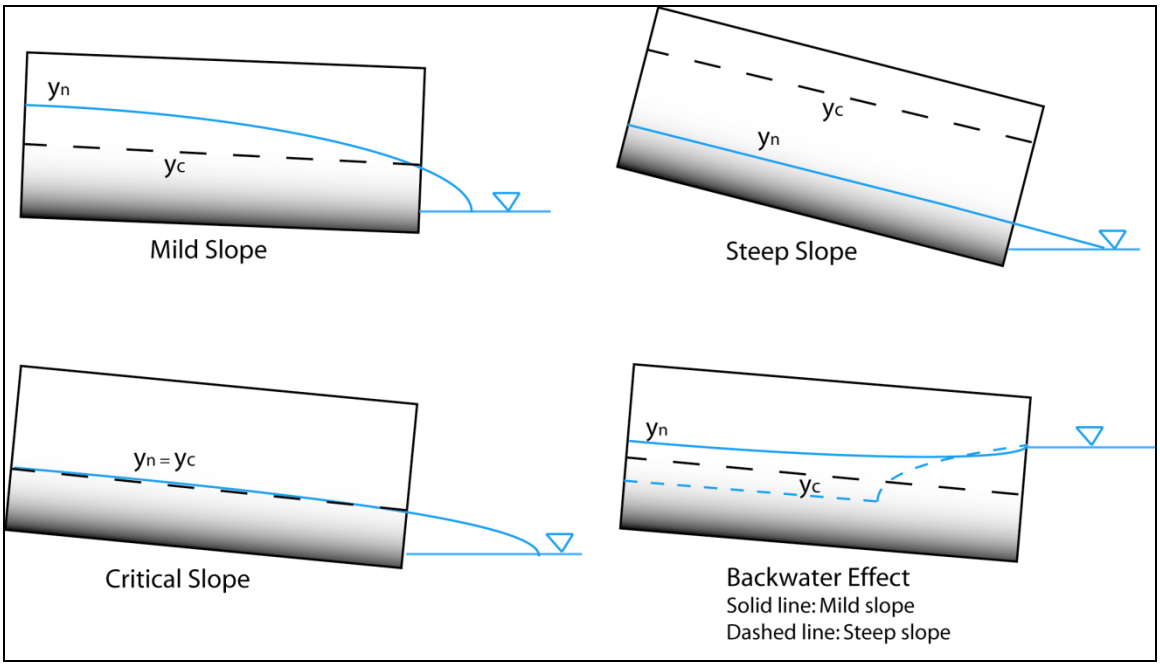

Figure 3. Permissible pipe exit conditions.

If the system is obeying conservation of momentum and the length of pipe is sufficient such that the friction slope is equal to the bed slope, the solved depth should be normal depth. Critical depth, however, must be calculated for the given flow rate and geometric variables. As the solution for critical depth is non-linear, the Newton-Raphson iterative solution technique was employed. This method searches for roots of an equation with a truncated Taylor series expansion to approximate $F(x)$ for some estimate of x. In this case, the function $F(x)$ is Manning's equation for open channel flow (Equation 10.) Because the series is truncated, the solution is not perfect. A correction is applied by Equation 11, where Δx is a correction to flowrate Q.

$$Q = \frac{1}{n} A R^{2/3} S_0^{1/2} \tag{10}$$

$$\Delta x = -\frac{F(x)}{\partial F / \partial x} \tag{11}$$

Iterations are performed until the correction Δx drops below a given threshold (1E-8). This process was imbedded into the code, and at each time-step the exit depth is checked against both critical depth and downstream junction depth.

Model Verification. To verify that the complete model was operating properly, Ji's (1998) test simulation for a simple six pipe network was reproduced.

Changes to Model. The nature of Equations 8 and 9 does not allow flow to move into the system when the area of flow is zero. It is therefore necessary to maintain a very small depth at the nodes even when flow is zero. Imposing a depth may create a numerical instability within the flow calculation, as physically these numbers should be generated simultaneously. Extensive testing found that an initial depth of 0.00001 m provided a stable minimum, allowing flow to commence without significantly affecting the mass and energy balance. This value is likewise imposed when inputs cease and a network drains, simply effectively keeping the pipes "wet".

Linking Models. Interaction between GSSHA and the subsurface is allowed to occur by controlling the end boundary conditions for SUPERLINKS. Inflow to the subsurface is permissible via culverts and grate openings in the roadway. The potential inflow to the subsurface network (q_{in}) in each node is given as a percentage of the total ponded volume (V_{ponded}) in the GSSHA grid cell per time step (dt) and the number of grates per node (N = 1 to 4)

$$q_{in} = \frac{N \alpha V_{ponded}}{dt} \tag{12}$$

where $\alpha = 1/N_{max}$. This conceptualization is necessitated by the fact that GSSHA planar grid cells are not typically small enough to accurately describe the micro-topography of curb depressions on crowned roadways where grates are typically located. It is further assumed that a cell with four grates would be capable of intercepting all ponded water for grid sizes on the order of 10 to 30 m. At each time step SUPERLINKS determines if there is sufficient capacity to accept from the inlet structures. If there is not sufficient space, the flow will be forced to remain on the overland flow plane.

Any manholes containing heads greater than the ground surface elevation will result in a transfer of volume out of the storm drainage network into the GSSHA overland flow plane. Discharge to channels can occur from any specified outlet pipe and is explicitly calculated at each time step. For complete details of SUPERLINKS and subsequent GSSHA integration the reader is referred to Ji (1998) and Zahner (2004).

Dead Run Watershed - Baltimore, Maryland Application.

It was necessary to model a watershed with a significant urban presence and subterranean drainage network to fully test the routines. A low gradient topography would provide situations of inundation and pressurized pipes. But perhaps most critical was the availability of a quality dataset including: rainfall records, stream flow records, digital elevation model (DEM), land-use coverage, stream channel, and storm drainage network data. Dead Run, a 14.3 km^2 watershed in Baltimore, Maryland, readily met these requirements. Drainage networks in urban watersheds are typically channelized or buried (using a sub-surface pipe network,) significantly altering the natural layout, such as those found in Dead Run (Figure 4). To correctly include the effects of these changes to the natural drainage network, the storm drainage networks must be explicitly considered in the model formulation. GSSHA model parameters were aggregated to a 30.0 m grid resolution based on land use/cover and soil GIS layers. Based on the classification that covers the majority of the grid cell, parameters such as porosity, roughness, saturated hydraulic conductivity, capillary head, and initial soil moisture were assigned. Impervious surfaces cover approximately 35 percent of Dead Run, as shown in the 30.0 m gridded land use map (Figure 5) used to assign GSSHA model parameters. Soils, DEM, and Land Use data came from Baltimore County.

Modeling Application. The storm drainage network will have its most pronounced effect during a moderate to high intensity storm. Hurricane Isabel passed over the area September 18-19, 2003 and was selected as the model test case. The storm dropped heavy rainfall on much of the east coast, including Maryland and the Baltimore watershed of Dead Run. As is common in hurricane precipitation patterns, Baltimore received two strong pulses of rainfall 150 minutes apart. The peak discharge recorded by the USGS gauging station at the outlet of the watershed was just under 40 cms. Basin averaged rainfall peaked at 53 mm/hr, but localized cells of intense precipitation were estimated by radar above 200 mm/hr. Thus, the distributed nature of the rainfall input is as critical as the distributed land use and soil classification. This event was also selected because it allows calibration of GSSHA using the observed precipitation and stream records.

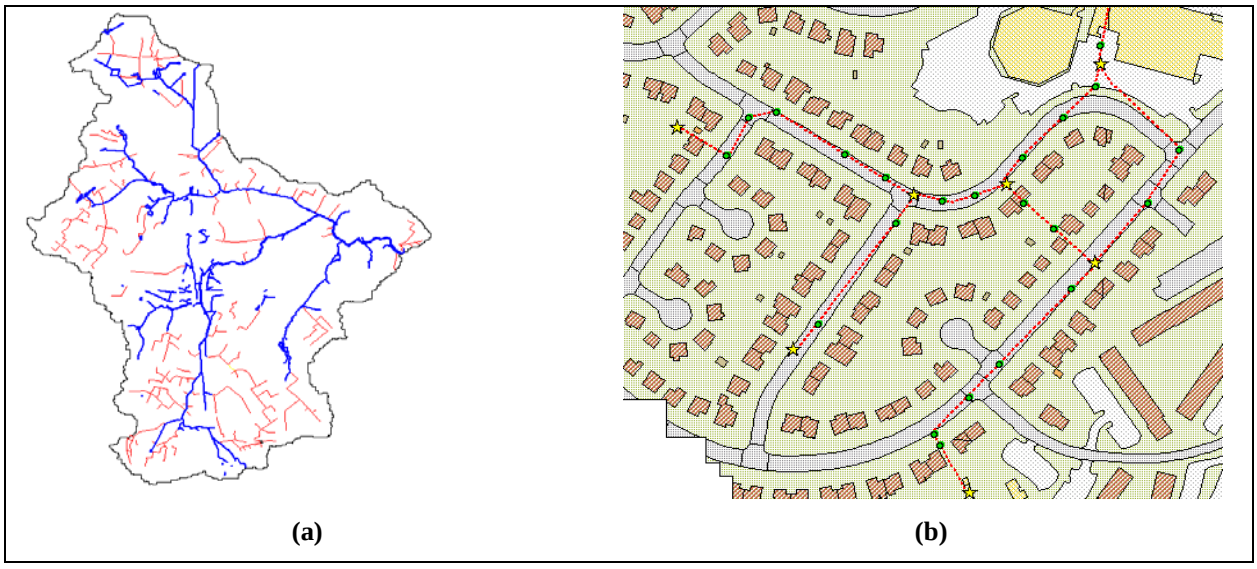

Figure 4. Part A demonstrates the existing natural channel network in blue (bold lines) and the storm drainage network in red (thin lines.) Part B shows the digitized drainage network (red lines) with locations of inlet grates (green dots) and junction locations (yellow stars).

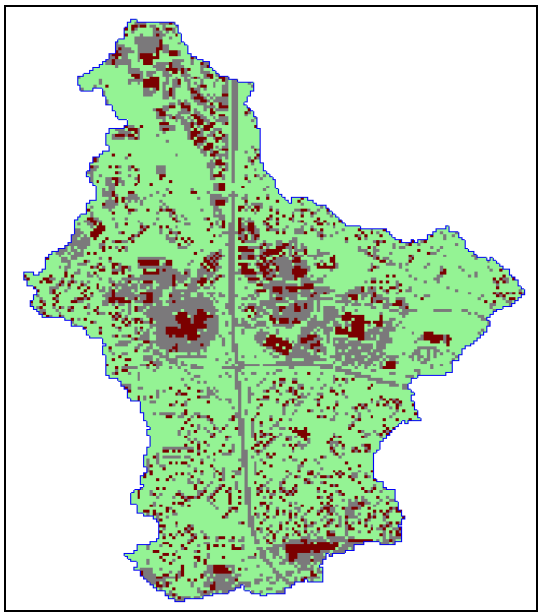

Figure 5. 30.0 m gridded land use map used to assign model parameters; forested areas are shown in green, roads and sidewalks in gray, and buildings in dark red.

Calibration: A manual calibration was performed by comparing the GSSHA outflow hydrograph to the USGS observed discharge record at the basin outlet. Saturated hydraulic conductivity ($K_{sat,}$) was varied between 0.1 and 0.8 cm/hr as simulation results were compared to the observed plot. Figure 6 displays the final simulation with a K_{sat} value of 0.5 cm/hr. The model is most sensitive to $K_{sat,}$ and the final value was chosen for its ability to produce a first peak of approximately 40 cms.

Table 1. Dead Run final parameter set.

Parameter	Value
Roughness	
Grassy, Natural Areas	0.40
Roadways, Parking Lots	0.05
Rooftops	0.80
Channels	0.04
Initial Soil Moisture	Saturated
Sat. Hydraulic Conductivity	0.50*

Note: values with * were calibrated.

Scenario Analysis: With the model fully set up, it is possible to simulate several different conditions to more fully understand the impact of storm drainage networks and other aspects of urbanization on how the watershed will respond to storm events. Three different sets of scenarios were looked at: pre- and post- urbanization analysis, storm drainage v. impervious area analysis, and a test of storm drainage impact on a more extreme event.

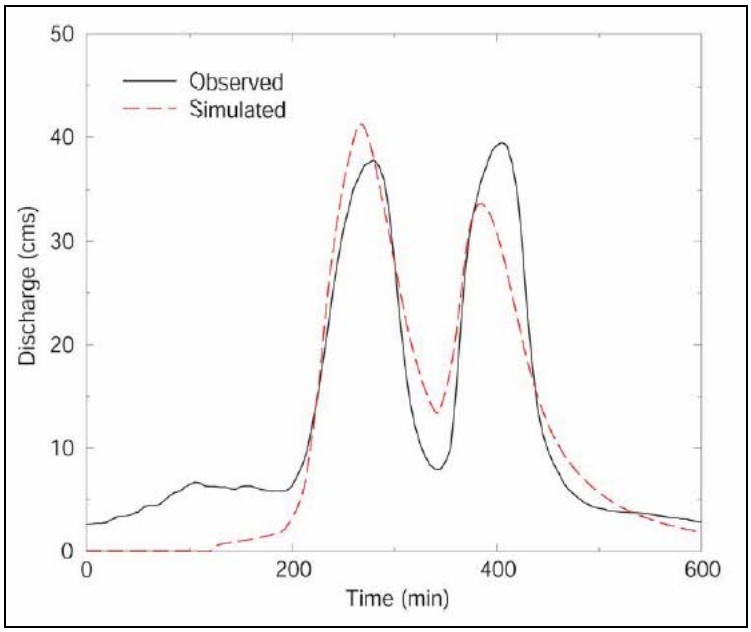

Figure 6. Final output hydrograph from manually calibrated model.

Urbanization Effect Analysis: This analysis was done to examine pre- and post-development conditions. Simulating the pre-development watershed is clearly a subjective task. It is impossible to reproduce every hydrologic feature that existed prior to development. There are some approximations, however, that can be made based on typical development trends and existing topography.

The channel network for this simulation was derived from a flow accumulation algorithm. The width and depth of these "natural" channels were assigned identical values to the modified network to avoid storage-related differences. The one property given a slightly different value was the roughness coefficient. Urbanized channel networks often are intensively maintained, reducing flow attenuating material such as brush and long grass which might persist in a natural channel. They also tend to be straighter and more efficient than a naturally formed channel. Thus, a Manning's N of 0.04 was used rather than 0.05, as recommended by Chow et al. (1988).

Three networks were simulated without the existing impervious areas so as to remove land surface factors from influencing a strictly channel comparison. Figure 7 shows the results of three conditions: "natural" channels, an expanded channel network as exists currently, and a current channel network with existing detention basins and culverts.

The results of this scenario clearly show the direct impact of the channel modifications on the natural hydrograph, with the result being a significant increase in peak flow. While the addition of on-line storage basins did decrease the peak flow, the effect is still overwhelmed by the storm drainage network impact when compared to the pre-development condition.

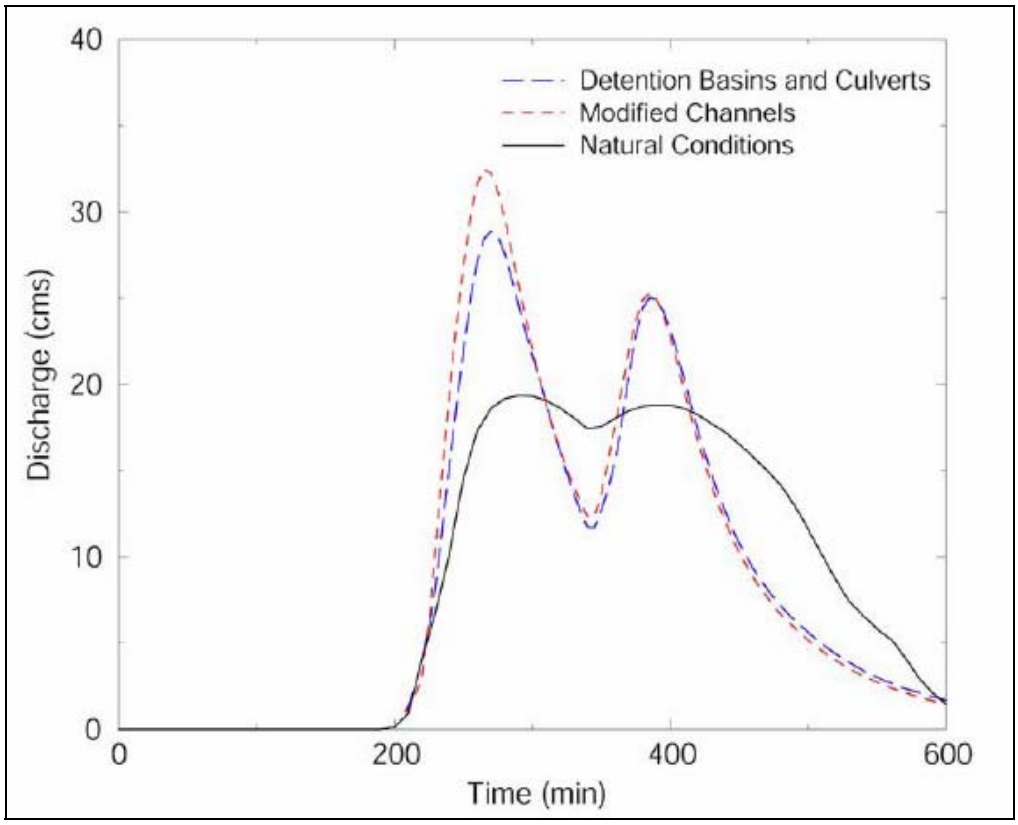

Figure 7. Output hydrograph comparison from three urbanization scenarios. None of these scenarios include the effects of impervious areas so that only the effect of the stream channels can be judged.

Storm Sewer versus Impervious Area Analysis: With the storm sewers fully functional, it is possible to explore the relative effect of various model components. To assess the question of impervious coverage versus storm sewers, Figure 8 contains plots of sequentially added impervious areas and storm sewers. *Case 1:* no impervious areas, no storm sewer; *Case 2*: distributed impervious areas, no storm sewer; *Case 3*: distributed impervious areas with storm sewer network. All cases include the same channel network, detention basins, and culverts.

Once again, the results show a significant impact due to increasing the drainage density by the addition of storm drains to a watershed over and above the impact of increased impervious area. The storm drainage network increases the peak flow significantly for the event.

Extreme Event Analysis: To fully explore the hypothesis that storm sewers become overwhelmed and have less of an effect on extreme events, polarimetric radar-rainfall estimates from the 1997 event that caused flash flooding in Fort Collins, Colorado (Ogden et al. 2000) were simulated over the Dead Run watershed. In this simulation on Dead Run, this four-pulse storm resulted in 15 cm (7.9 in) of rain in 4 ½ hours, more than doubling the flood peak of the Dead Run outlet hydrograph compared to Hurricane Isabel. Although the drainage of the basin was slightly enhanced, as seen in Figure 9, the flood magnitude was practically unaffected. The limited conveyance and intake potential of the drainage network could not enhance flow routing to the outlet enough to raise the peak discharge.

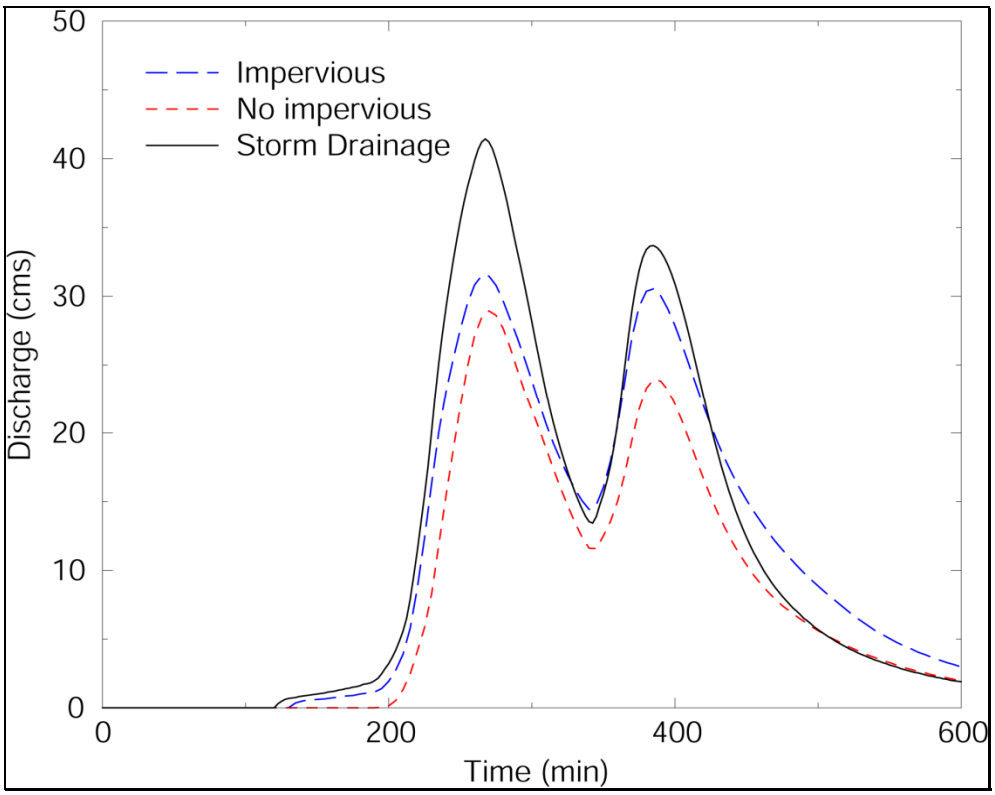

Figure 8. Comparing the effect of imperviousness vs. storm sewer. The storm drainage network showed a marked increase in peak runoff from the base condition (no impervious area) compared to the addition of impervious area.

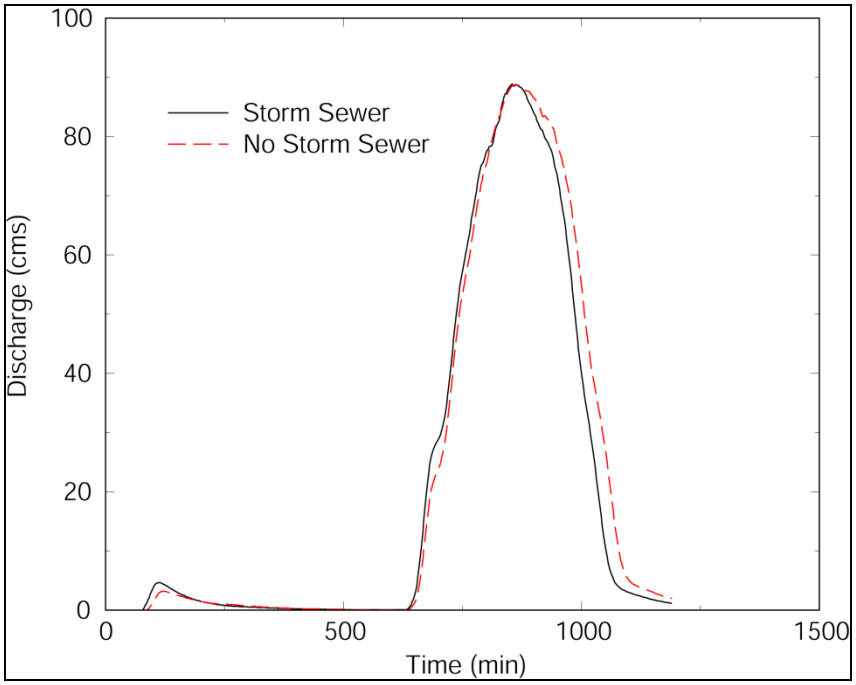

Figure 9. Reduced effect of storm sewers with extreme event.

CONCLUSIONS. Urban flooding is caused by many factors, one of which is the increase in hydraulic pathways due to an increase in storm drainage networks. In examining the effects of storm drainage systems it is evident that moderate storm drainage systems have a significant impact on flood magnitude and timing for moderate to high precipitation events but an almost negligible effect on extreme events, such as extreme-precipitation hurricanes. When compared to the effects of impervious land surface for the moderate to high events, the storm drainage network had a much more significant impact on increasing the downstream flood peak than the impervious land surface. These results have a direct impact on engineering a solution for flooding in an urban setting. The results also show that GSSHA is able to reproduce the effects of storm drainage systems on flood timing and magnitude and can thus be used in an engineering setting.

ADDITIONAL INFORMATION: This technical note was prepared by Aaron Byrd, research hydraulic engineer, Coastal and Hydraulics Laboratory, U.S. Army Engineer Research and Development Center. The study was conducted as an activity of the Regional Watershed Modeling and Management work unit of the System-Wide Water Resources Program (SWWRP). For information on SWWRP, please consult *https://swwrp.swwrp.army.mil/* or contact the Program Manager, Dr. Steven L. Ashby at *Steven.L.Ashby@erdc.usace.army.mil.* This technical note should be cited as follows:

> Ogden, F. L., J. M. Niedzialek, and A. R. Byrd. 2012. "Storm drain effects on urban flooding," *SWWRP Technical Notes Collection*, ERDC TN-SWWRP-12-1, U.S. Army Engineer Research and Development Center, Vicksburg, MS. *https://swwrp.usace.army.mil/*

REFERENCES

Chow, V. T., D. R. Maidment. 1988. *Applied Hydrology*. New York, McGraw-Hill, Inc.

Downer, C. W. and F. L. Ogden. 2006. Gridded Surface Subsurface Hydrologic Analysis (GSSHA) User's Manual, Version 1.43 for Watershed Modeling System 6.1. Vicksburg, System Wide Water Resources Program, Coastal and Hydraulic Laboratory**:** 207.

Franz, D. D., and C. S. Melching. 1997. Full Equations (FEQ) model for the solution of the full, dynamic equations of motion for one dimensional unsteady flow in open channels and through control structures. W. R. I. Report, U.S. Geological Survey 258.

Gustafsson, L.-G., C. Hernebring. 1999. *Continuous Modelling of Inflow/Infiltration in Sewers with MouseNAM - 10 Years of Experience*. 3rd DHI Software Conference, Helsingør, Denmark.

Ji, Z. 1998. "General Hydrodynamic Model for Sewer/Channel Network Systems." *Journal of Hydraulic Engineering* 124(3): 307-315.

Lewis, J. M., D. L. Fread. 1996. *An extended relaxation technique for unsteady flows in networks*. North American Water and Environment Congress, Reston, VA, ASCE.

Ogden, F. L., H. O. Sharif. 2000. "Hydrologic analysis of the Fort Collins, Colorado, flash flood of 1997." *Journal of Hydrology* 228(1-2): 82-100.

Rossman, L. A., R. Dickinson. 2004. SWMM 5 - the Next Generation of EPA's Storm Water Management Model. *Innovative Modeling of Urban Water Systems*. W. James. Guelph, Ontario, CHI. Monograph 12.

Smith, J. A., M. L. Baeck. 2002. "The Regional Hydrology of Extreme Floods in an Urbanizing Drainage Basin." *Journal of Hydrometeorology* 3(3): 267-282.

Zahner, J. A. 2004. Influence of Storm Sewers, Drainage Density, and Soil Moisture on Runoff From an Urbanizing Catchment. *Civil and Environmental Engineering Department*. Storrs, University of Connecticut. M.S. Thesis.